1028 *KSME International Journal, Vol. 14, No. 10, pp. 1028~1040, 2000*

A Numerical Method for Dynamic Analysis of Tracked Vehicles of High Mobility

Kisu Lee*

Associate Professor, Department of Mechanical Engineering, Chonbuk National University

A numerical method is presented for the dynamic analysis of military tracked vehicles of high mobility. To compute the impulsive dynamic contact forces which occur when a vehicle passes on a ground obstacle, the track is modeled as the combination of elastic links interconected by pin joints. The mass of each track link, the elastic elongation of a track link between pin joints by the track tension, and the elastic spring effects on the upper and lower surfaces of each track link have been considered in the equations of motion. And the chassis, torsion bar arms, and road wheels of the vehicle are modeled as the rigid multibodies connected with kinematic constraints. The contact positions and the contact forces between the road wheels and track, and the ground and the the track are simultaneously computed with the solution of the equations of motions of the vehicle consisting of the multibodies. The iterative scheme for the solution of the multibody dynamics of the tracked vehicle is presented and the numerical simulations are conducted.

Key Words : Tracked Vehicle, Vehicle Dynamics, Contact Force

1. Introduction

Even though computational multibody dynamics are widely used for the dynamic analysis of various kinds of machines and vehicles (e. g., Garcia de Jalon and Bayo, 1994), the application to the tracked vehicles is relatively limited. The major difficulties in analyzing the tracked vehicles by the computational multibody dynamics are the efficient and realistic modeling of the track and the accurate computation of the contact forces acting on the track. Literature survey shows that the track is usually regarded as massless internal force elements between the road wheel and the ground. For example, McCullough and Haug (1986) represented the track as the internal force elements and assumed that the track is connected by the several straight lines between the road wheels or between the road wheel and the obstacle. But, in most of the real tracked vehicles of high mobility, the track makes point contact with the road wheel due to high track tension, and the track cannot be represented by several straight lines because the inertia effects of the track cannot be neglected when impulsive contact forces developed by the obstacles on the ground (it is worth to note that, in most of the military tracked vehicles, the total weight of the track is almost equal to the total weight of the road wheels). Meanwhile, Nakanishi and Shabana (1994) investigated the dynamics of the tracked vehicles such as bulldozers and hydraulic excavators with full consideration of inertia effects of the track. They represented the track as the rigid bodies interconnected by revolute joints and computed the contact forces between the track and the road wheels, rollers, sprocket, and idler with the suitable values of the stiffnesses of the springs. They included the rotary inertia of the track link in the equation of motion and solved the mixed differential algebraic equations.

* **E-mail** : kisulee@moak.chonbuk.ac.kr
TEL : +82-63-270-2326 ; **FAX** : +82-63-270-2315
Department of Mechanical Engineering, Chonbuk National University, Chonju, Chonbuk 561-756, Korea.(Manuscript **Received** October 16, 1999 ; **Revised** April 27,. 2000)

Even though such a modeling technique might be applicable for the tracked vehicles of low velocity having negligible track tension, to the author's best knowledge, for the military tracked vehicles having large track tension, the rotary inertia of the track link may be neglected compared to the relatively larger translatory inertia of the track link. And efficient numerical techniques should be adopted to enforce the correct contact constraints on the track because very large contact forces usually play the major roles in the military tracked vehicles of high mobility especially when they pass the obstacles with high velocity. Also, the track tension should be involved in the equation of motion and should be simultaneously computed with the other unknowns of the equation of motion.

In this work, the dynamic problems of military tracked vehicles are solved by combining the numerical techniques suggested by the author for multibody dynamics (Lee, 1993) and dynamic interaction between the vehicle and the flexible structure (Lee, 1997), respectively. To compute the correct dynamic contact force acting impulsively, the track is modeled as the combination of elastic links interconnected by pin joints. The mass of each track link, the elastic elongation of a track link between pin joints by the track tension, and the elastic spring effects on the upper and lower surfaces of each track link have been considered in the equations of motion. And the chassis, torsion bar arms, and road wheels of the vehicle are modeled as the rigid bodies connected with kinematic constraints. The Lagrange multipliers associated with the kinematic constraints of the vehicle components, the contact forces acting on the track, and the track tension are simultaneously computed with the equation of motion of the whole system. In this work the modeling techniques of the tracked vehicle for computing the dynamic contact forces acting impulsively on the track and road wheels are explained, and the numerical simulations are conducted.

2. Modeling of Tracked Vehicles and Contact Forces

2.1 Modeling of vehicle and track

In this work, two-dimensional military tracked vehicles of high mobility are considered with special attention on the impulsive contact forces acting on the track and road wheels. The vehicle is assumed to consist of rigid chassis (i. e., hull and turret), rigid road wheels, rigid torsion bar arms, and track. And the rigid torsion bar arms are connected to the chassis of the vehicle by the torsion bar springs. In the tracked vehicles, among the contact forces between the track and the vehicle components, the contact forces between the track and the road wheels play the major roles. Thus, for the sake of simplicity, the sprocket, idler, and roller supports are not considered in this work, and the both ends of the track are directly connected to the chassis as shown in Fig. 1. In this work the rotary moment of inertia of each road wheel about its center is neglected, and thus the road wheel and the torsion bar arm are regarded as one continuous rigid body. Also, the friction between the road wheel and the track is neglected (the vehicle is assumed to move with a constant horizontal velocity at the beginning of the analysis), and thus the contact force acting on the road wheel directs toward the center of the road wheel. The kinematic constraints between the chassis and the torsion bar arms are generally expressed as

$$\Phi(q, t)=0 \tag{1}$$

where q is the vector of the generalized coordinates of the multibodies consisting of the chassis and the connected vehicle components, and t denotes the time.

When a tracked vehicle collides with a large

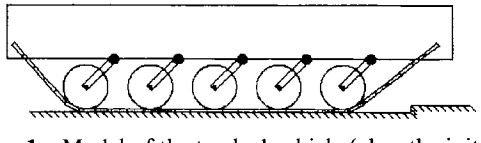

Fig. 1 Model of the tracked vehicle (also, the initial configuration for the numerical experiment)

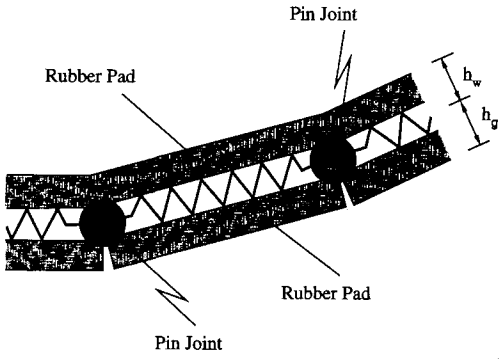

Fig. 2 Model of the track

ground obstacle, the shape of the track usually changes drastically by the impulsively forces. Thus, for the correct dynamic analysis, it is essential to compute the complicated track shapes after the impulsive collision. In this work, for computing the contact forces acting impulsively on the track, the track is assumed to consist of the links interconnected by pin joints as shown in Fig. 2. As the length of the track link is relatively small in the real tracked vehicles, the rotary inertia of each link is neglected, and the mass of the track is assumed to be concentrated on the pin joints. In the real military tracked vehicles the track links are made of thick steels, and the pin joints between the track links are covered by elastic rubber bushes which deform by track tension. Also, the upper and lower surfaces of the track links are covered by thick elastic rubber pads in the real military tracked vehicles. Thus, in this work, for the elastic effects of the track center line in the longitudinal directions of the links due to the rubber bushes on the pin joints, the track links are assumed to be massless stiff springs which may be deformed in the longitudinal directions between the pin joints (the springs between the pin joints maintain straight lines during the deformation). As the rubber pads on the upper and lower surfaces of the track link may deform by the contact with the road wheel and the ground, respectively, the stiff springs are assumed to exist on the contact points of the upper and lower surfaces of the track. In this work the ground is assumed to be a rigid body, and the surface of the ground is expressed by using several

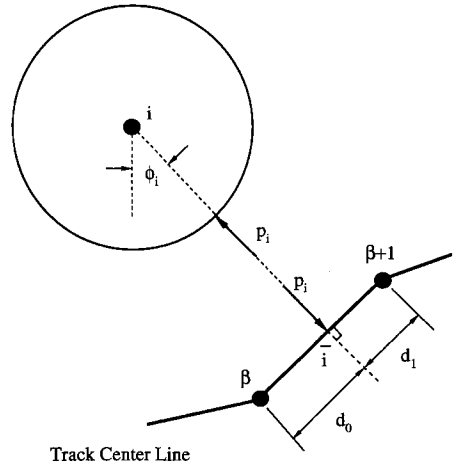

Fig. 3 Possible contact points between the wheel and the track link

lines. The vehicle is assumed to move on the ground without friction.

2.2 Contact points and contact forces of track

The road wheels of the vehicle may contact with the track, and the track may contact with the ground as explained before. The huge contact forces developing on such contact points usually govern the equations of motion of the whole system. Thus special techniques are required to detect the correct contact points and to compute the correct contact forces in the solution. In this work, by the same way explained by Lee (1997), the possible contact points between the road wheel and the track are detected by drawing the normal line from the center of the road wheel to each link of the track as shown in Fig. 3. Then, for the wheel shown in Fig. 3, the distance between the wheel center i and the corresponding center line of the track link, s_i, is
expressed as

$$s_i = -(w_{ix} - u_{ix})\sin\phi_i + (w_{iy} - u_{iy})\cos\phi_i \quad (2)$$

where w_{ix} and w_{iy} are the coordinates of the center of the road wheel i which are easily obtained from generalized coordinates q of the vehicle, and ϕ_i is the angle denoting the normal direction as shown in Fig. 3. Also, u_{ix} and u_{iy} are the coordinates of point $\bar{i}$ in the center line of the

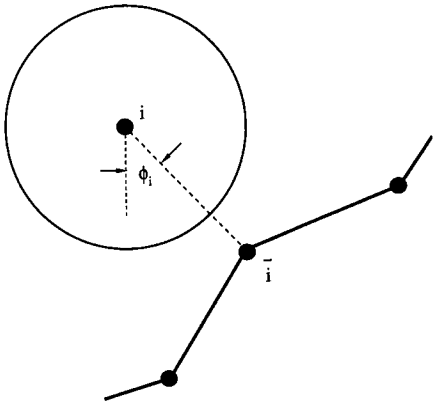

Fig. 4 Possible contact points between the wheel and the pin joint of the track

track link shown in Fig. 3 which are related to the coordinates of pin joints β and $(\beta+1)$, $a_{\beta x}$, $a_{\beta y}$, $a_{(\beta+1)x}$, and $a_{(\beta+1)x}$, by the following:

$$u_{ix}=\frac{d_1 a_{\beta x}+d_0 a_{(\beta+1)x}}{d_0+d_1}$$
$$u_{iy}=\frac{d_1 a_{\beta y}+d_0 a_{(\beta+1)y}}{d_0+d_1} \qquad (3)$$

where d_0 and d_1 denote in Fig. 3 (they are determined by drawing the normal lines on the track center line). And, if the track links are positioned as shown in Fig. 4, the normal lines from the center of the wheel does not intersect with the track links even though the pin joint between them may contact with the wheel. In such a case, as shown in Fig. 4, the line connecting the wheel center and the pin joint is regarded as the normal line on which the contact force is acting. The contact force between the road wheel and the track may be computed by using the compression of the rubber pad between them. For example, if the contact force is assumed to be linearly related to the deformation, the contact force acting on possible contact point i, p_i may be written as

$$p_i=\max\{k_w(r+h_w-s_i),\ 0\} \qquad (4)$$

where k_w is the spring constant of the rubber pad between the track and wheel, r is the radius of the road wheel, and h_w is the distance between the upper surface of the track and the center line of the track as shown in Fig. 2.

The possible contact points between the track

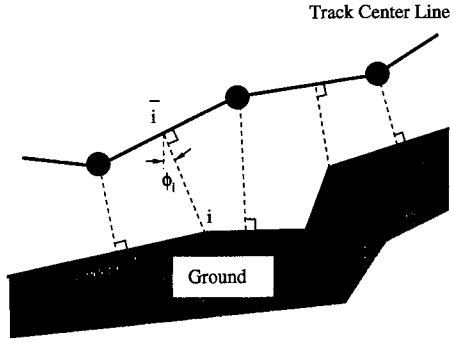

Fig. 5 Possible contact points between the ground and the track link

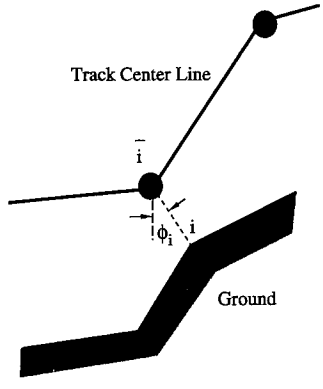

Fig. 6 Possible contact points between the corner of the ground and the pin joint of the track

and the ground may be detected by drawing the normal lines from the pin joints of the track to the ground, and also by drawing the normal lines from the corner points of the ground to the track links as shown in Fig. 5. For the ith possible contact point shown in Fig. 5, the distance between the center line of the track and the possible contact point on the ground, s_i, is expressed as

$$s_i=-(u_{ix}-x_{ix})\sin\phi_i+(u_{iy}-x_{iy})\cos\phi_i \qquad (5)$$

where u_{ix} and u_{iy} denote the coordinates of point $\bar{i}$ on the track center line shown in Fig. 5 and may be computed by the relation similar to (3), x_{ix} and x_{iy} denote the coordinates of possible contact point i on the ground, and ϕ_i is the angle denoting the normal direction shown in Fig. 5. If the track links are positioned as shown in Fig. 6, the normal lines from the corner point of the ground does not intersect with the track links

even though the pin joint between them may contact with the corner of the ground. In such a case, as shown in Fig. 6, the line connecting the corner of the ground and the pin joint is regarded as the normal line on which the contact force is acting. The contact force between the ground and the track may be computed by using the relative deformation between them. Even though such contact force is usually nonlinearly related to the compressed deformation on the contact point, if linear relation is assumed for the sake of simplicity, contact force acting on possible contact point i, p_i, may be written as

$$p_i=\max\{k_g(h_g-s_i),\ 0\} \tag{6}$$

where k_g is the spring constant between the track and the ground, and h_g is the distance between the lower surface of the track and the track center line as shown in Fig. 2. Even though damping effects may also be accompanied when the rubber pads are deformed by the contact forces, for the simplicity, the damping related to the track deformation is not included in the equations.

3. Equation of Motion

In this work, the equation of motion of the multibodies connected to the chassis with kinematic constraints (i. e., the equation of motion of the vehicle except the track) is written with the generalized coordinates which are widely used in multibody dynamics. As the masses of the track links are assumed to be concentrated on the pin joints, the equations of motions of the track are simply written with the global x and y coordinates. In the equation of the multibodies including the chassis and the road wheels, the contact forces acting on the road wheels are easily transformed to the generalized forces corresponding to generalized coordinates q by the basic principles of the dynamics. In the equations of the track, the contact force acting on the track link is decomposed into the equivalent forces acting on the adjacent pin joints. For example, in Fig. 3, contact force p_i acting on the track is decomposed into equivalent forces p'_β and $p'_{\beta+1}$ acting on pin joints β and $\beta+1$ by the following:

$$p'_\beta=\frac{d_1}{d_0+d_1}p_i$$
$$p'_{\beta+1}=\frac{d_0}{d_0+d_1}p_i \tag{7}$$

The track tension may be computed by using the deformations between the pin joints. For example, if the spring in the center line of the track link in Fig. 2 is assumed to be linear, track tension $T_{\beta(\beta+1)}$ between pin joints β and $\beta+1$ may be computed by the following:

$$T_{\beta(\beta+1)}=k_\tau(\sqrt{(a_{\beta x}-a_{(\beta+1)x})^2+(a_{\beta y}-a_{(\beta+1)y})^2}-L_0) \tag{8}$$

where k_τ is the spring constant which is assumed to exist in the center line of the track, $a_{\beta x}$, $a_{\beta y}$, $a_{(\beta+1)x}$, and $a_{(\beta+1)y}$ denote the deformed coordinates of pin joints β and $\beta+1$, respectively, and L_0 denotes the undeformed length of the track link.

The equation of motion of the whole vehicle may be written as

$$\begin{bmatrix} M_c & 0 \\ 0 & M_\tau \end{bmatrix}\begin{bmatrix} \ddot{q} \\ \ddot{a} \end{bmatrix} = \begin{bmatrix} -\Phi_q^T\lambda+Hp_w+c_c(q,\ a)+f_c \\ Q_w\ R_w\ p_w+Q_g\ R_g\ p_g+e(a)+c_\tau(q,\ a)+f_\tau \end{bmatrix} \tag{9}$$

where M_c is the mass matrix of the multibodies consisting of the chassis and the connected bodies, and M_τ is the mass matrix of the track, q is the vector of generalized coordinates of the chassis and the connected bodies, a is the vector of the x and y coordinates of the pin joints of the track, Φ_q is the constraint Jacobian matrix, and λ is the vector of Lagrange multipliers. p is the vector of the contact forces between the rigid road wheels and the track, and the track and the grounds. H is the matrix transforming the contact forces to the generalized forces corresponding to coordinates q, R is the matrix transforming the forces acting on the contact points to the equivalent forces acting on the pin joints of the track (cf., Eq. (7)), and Q is the matrix transforming the normal contact forces p on the contact points to the x and y components of the global coordinates. Subscripts w and g denote the contact

between the road wheel and the track, and the ground and the track, respectively (e.g., p_w means the contact force acting between the wheel and the track, and p_g means the contact force acting between the wheel and the ground). And $e(a)$ is the vector of the forces by the track tension (cf., Eq. (8)), and $c_c(q, a)$ and $c_\tau(q, a)$ are the forces acting on the chassis and the track at the both ends of the track by the track tension. f_c and f_τ are the vectors of the known forces such as gravity acting on the chassis and track, respectively.

4. Solution Strategy

4.1 General consideration and constraint error vectors

For the solution of this work, differential Eq. (9) and algebraic Eq. (1) should be solved simultaneously. Further, the correct contact positions between the road wheels and the track, and the ground and the track should be simultaneously detected with the solution. In this work, by employing the iterative scheme of Lee (1993, 1997) which will be explained in the next section, the correct value of Lagrange multiplier λ which makes constraint Eq. (1) be satisfied is computed at each time step. And the correct contact positions are detected by drawing the normal lines as shown in Figs. 3-6 at each iteration of each time step. Then, Eq. (9) becomes an ordinary differential equation without any constraint, and a well-established time integration techniques of ordinary differential equation can be easily employed. Thus, the basic strategy of this work is to find the correct Lagrange multipliers and correct contact positions at each time step by iterations and to solve ordinary differential Eq. (9) with these known Lagrange multipliers and contact positions. In this work, the one step method is employed for the time integration, and hence the complicated discontinuous motion due to the impacts between the track and the road wheels, and between the track and the ground may be efficiently computed (e. g., Addison, Enright, Gaffney, Gladwell, and Hanson (1991), and Cash and Karp (1990)).

For the dynamic analysis of the multibodies, besides holonomic constraint Eq. (1), the following differential constraints should also be satisfied on the kinematic joints:

$$\Phi_q \dot{q} + \Phi_t = 0, \tag{10}$$

$$\Phi_q \ddot{q} + (\Phi_q \dot{q})_q \dot{q} + 2\Phi_{qt}\dot{q} + \Phi_{tt} = 0 \tag{11}$$

In this work, constraint Eqs. (1), (10), and (11) are called as position constraint, velocity constraint, and acceleration constraint, respectively. In the practical computation, the satisfaction of one kind of constraints among constraint Eqs. (1), (10), and (11) does not guarantee the satisfactions of the other kinds of constraints and special techniques are required to make all the three kinds of the constraints be satisfied. For this purpose, by following the procedures of Lee (1993, 1997), constraint Eqs. (1), (10), and (11) are controlled by the corresponding constraint error vectors defined below.

1. In case of position constraint, constraint error vector v is defined as

$$v = -\Phi \tag{12}$$

2. In case of velocity constraint, constraint error vector v is defined as

$$v = -\Phi_q \dot{q} - \Phi_t \tag{13}$$

3. In case of acceleration constraint, constraint error vector v is defined as

$$v = -\Phi_q \ddot{q} - (\Phi_q \dot{q})_q \dot{q} - 2\Phi_{qt}\dot{q} - \Phi_{tt} \tag{14}$$

In the iterative scheme which will be explained in the next section, depending on the specified constraint required for that procedure, only one kind of the constraint error vector is selected among the three kinds of constraint error vector show in Eqs. (12)-(14).

The basic solution procedure of this work at each time step is essentially the same as that of Lee (1993, 1997) and briefly summarized in the following:

1. Solve Eqs. (9) and (1) by time integration, and determine q, Φ_q, a, $\dot{a}$, and $\ddot{a}$ of the time step (contact force p, transformation matrices H, Q, and R, and track tension are determined here during the time integration, and $\dot{a}$ and $\ddot{a}$ of the time step are also determined here because the equation of motion of the track is not subjected to constraint Eq. (1)).

2. Compute the integration error after solving Eqs. (9) and (1) with the half step size.

3. Solve Eqs. (9) and (10) to determine $\dot{q}$ of the time step.

4. Solve Eqs. (9) and (11) to determine λ and $\ddot{q}$ of the time step.

4.2 Iterative scheme

The correct Lagrange multipliers $\lambda^{t+\Delta t}$ at time step $t+\Delta t$ are computed by the following iterative scheme shown by Lee (1993, 1997):

$$\lambda^{t+\Delta T}=\lambda^{t+\Delta t, m-1}-\alpha A_n v^{t+\Delta t, m-1} / \|C\|_\infty \quad (15)$$

where m and $m-1$ are iteration counters, and α is a constant. A_n and C are matrices related to the solution acceleration and are explained in the Appendix and Eqs. (17)-(19) (unless a fast convergence of the iteration is required, A_n might be regarded as a unit diagonal matrix), And $v^{t+\Delta t, m-1}$ which is the constraint error vector corresponding to one of definitions in Eqs. (12)-(14) can be computed by using $q^{t+\Delta t, m-1}$, $\dot{q}^{t+\Delta t, m-1}$, and $\ddot{q}^{t+\Delta t, m-1}$ which are the solutions of Eq. (9) with λ replaced by $\lambda^{t+\Delta t, m-1}$. At each time step, the three different constraint error vectors are used to solve Eq. (9) and one of Eqs. (1), (10), and (11): position constraint error Eq. (12) is used when Eqs. (9) and (1) are solved, velocity constraint error Eq. (13) is used when Eqs. (9) and (10) are solved, and acceleration constraint error Eq. (14) is used when Eqs. (9) and (11) are solved. Iteration Eq. (15) is repeated until the corresponding constraint error vector becomes smaller than the prescribed tolerance.

When position constraint Eq. (1) is imposed by using position constraint error Eq. (12) in iterative scheme in Eq. (15), at each iteration of each time step, the contact points are determined by drawing the normal lines as shown in Figs. 3-6. Then, by the same way by Lee (1997), the correct contact points and the corresponding normal directions are detected as long as iterative scheme in Eq. (9) converges to the correct solution.

In the practical computation, because of the numerical errors involved in the numerical solutions of the equations of motion, the values of the Lagrange multipliers obtained by using constraint error vectors in Eqs. (12), (13), and (14), respectively, may not be the same. And the most accurate solution is obtained when acceleration constraint Eq. (14) is imposed in iterative scheme in Eq. (15) because numerical integration errors are involved in computing the velocities and the displacements. Thus the Lagrange multiplier computed by using acceleration constraint error Eq. (14) is regarded as the most accurate one and is used for the time integration in the subsequent time steps.

4.3 Computer implementation

As the present iterative method is essentially the same as those used by Lee (1993, 1997), the constraint error vectors are monotonically reduced if α is smaller than the specified value. Thus, in this work, only brief explanations required for the practical computation are given here (the detailed explanation on the convergence is shown by Lee (1993, 1997)). In iterative scheme (15), the optimum value of α is given as

$$\alpha=\frac{2}{w_n+\varepsilon_n} \quad (16)$$

where w_n and ε_n are quantities computed by definitions (A. 3) and (A. 4) in the Appendix by using a suitable value of n (for the accderated solution the value of n may be fixed (e. g., n=10) or may be controlled by the way shown by Lee (1989)) and matrix C defined below. When constraint error vector Eq. (12) is used in iterative scheme in Eq. (15), for the computation of w_n and ε_n, matrix C is given as

$$C=\frac{\Delta t^2}{6}\Phi_q M^{-1}\Phi_q^T \quad (17)$$

And, when constraint error vector Eq. (13) is used in iterative scheme in Eq. (15), matrix C is given as

$$C=\frac{\Delta t}{2}\Phi_q M^{-1}\Phi_q^T \quad (18)$$

Finally, when constraint error vector in Eq. (14) is used in iterative scheme in Eq. (15), matrix C is given as

$$C=\Phi_q M^{-1}\Phi_q^T \quad (19)$$

When $\overline{\varepsilon_1}$ in Eq. (A. 4) of the Appendix is required to be computed, n and α are set to be 1 and 1.9, respectively, in iterative scheme in Eq. (15), and $\overline{\varepsilon_1}$ is estimated by the initial J iterations (e. g., J=10) by the following way:

$$\overline{\varepsilon_1} = \min_{1 \le m \le J} \frac{1}{\alpha}\left(1 - \frac{\|v^m\|_2}{\|v^{m-1}\|_2}\right). \tag{20}$$

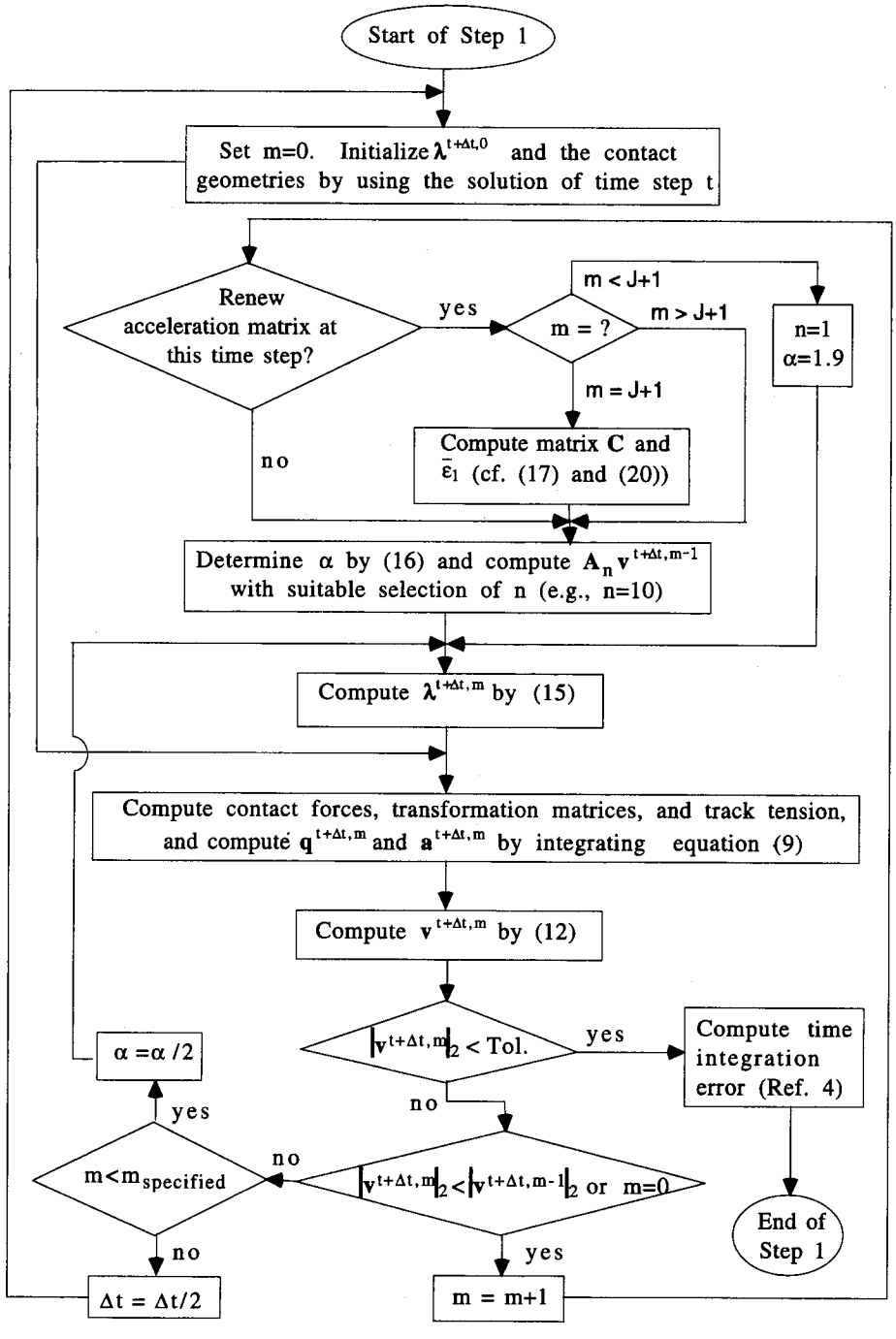

Fig. 7 Computing procedure of step 1 at time step $t+\Delta t$

The major tasks of this work are to compute λ, q, $\dot{q}$, $\ddot{q}$, a, $\dot{a}$, and $\ddot{a}$ at each time step by solving differential Eq. (9), constraint Eqs. (1), (10), (11), and the contact constraints on the track together. And the computation procedure at time step $t+\Delta t$ is explained below:

1. Solve Eq. (9) by imposing position constraint Eq. (1), and determine $q^{t+\Delta t}$, $a^{t+\Delta t}$, $\dot{a}^{t+\Delta t}$, and $\ddot{a}^{t+\Delta t}$, By following the procedures explained in Sec 2 and 3, contact force p, transformation matrices H, Q, and R, and track tension of time step $t+\Delta t$ are also determined here. Use iterative scheme in Eq. (15) with position constraint error vector in Eq. (12). The detailed procedure is shown in Fig. 7.

2. By the ways explained by Lee (1993), compute the total integration error of the equations of motion. If the total integration error is within the prescribed tolerance, predict the next step size by the way explained by Lee (1993), and go to step 3. Otherwise, go to step 1 to repeat the computation from the beginning of the current time step with the new step size.

3. By a procedure similar to step 1, with the contact force p, transformation matrices H, Q and R, and track tension determined at step 1, solve the upper part of Eq. (9) by imposing velocity constraint Eq. (10) and determine $\dot{q}^{t+\Delta t}$(the lower part of Eq. (9), i. e., the equation of motion of the track, need not be solved here because it does not contain a kinematic constraint of type (1)). Use iterative scheme in Eq. (15) with velocity constraint error vector in Eq. (13).

4. By a procedure similar to step 1, with the contact force p, transformation matrices H, Q and R, and track tension determined at step 1, solve the upper part of Eq. (9) by imposing acceleration constraint in Eq. (11) and determine $\lambda^{t+\Delta t}$ and $\ddot{q}^{t+\Delta t}$. Use iterative scheme in Eq. (15) with acceleration constraint error vector in Eq. (14)

5. Numerical Examples

In the numerical example of this section the tracked vehicle moves on the rigid ground having a step, and the initial configuration of the vehicle is shown in Fig. 1. The vehicle consists of a rigid chassis, five rigid torsion bar arms, five rigid road wheels, and track. The rotary moment of inertia of the road wheel with respect to its center is neglected, and the road wheel and the torsion bar arm are regarded to be a continuous body. The vehicle is equipped with the five torsion bar springs on which kinematic constraints (pin joints) between the chassis and the torsion bar arms are imposed. The data of the vehicle are: the mass and the moment of inertia of the chassis are 20,000kg and 47,700kgm^2, respectively, and the mass and the moment of inertia of each torsion bar arm including a road wheel are 300kg and 12. 5kgm^2, respectively. The length of each torsion bar arm is 0.5m, and the mass center of the torsion bar arm and road wheel is assumed to be located on the center of the road wheel. The relative x and y coordinates of the track ends are$(-2.81\text{m}, 0\text{m})$ and (2.54m, 0m), respectively, from the mass center of the chassis. The relative x and y coordinates of the first torsion bar are (1.7m, -0.2m) from the mass center of the chassis, and the distance between each torsion bar is 0.81m. The torsional spring constant of the torsion bar is 191kNm and each torsion bar makes 45° with the horizontal axis at the initial equilibrium state. The radius of the road wheel is 0.28m.

The track consists of 30 elastic links, and the data of each link are: the length in the undeformed state is 0.19m, the mass is 20kg, the spring constant in the longitudinal direction is 8×10^6N/m. The constants of the both springs between the road wheel and the track, and between the ground and the track are assumed to be 10^8 N/m, and h_w and h_g shown in Fig. 2 are taken to be 2cm. And the average track tension in the initial equilibrium state is 80.4kN(in the initial equilibrium state the highest track tension in front of the first road wheel is 84.18kN, and the lowest tension in the track touching the ground is 78.68kN). And the height of the step on the ground is 0.1m.

Initially the vehicle is in the equilibrium state as shown in Fig. 1 and moves with the horizontal velocity of 10 m/s, and touches the corner of the step of the ground at t=0.0568 sec. The configura-

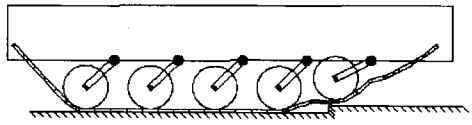

Fig. 8 Configuration of the tracked vehicle at t=0.1 sec

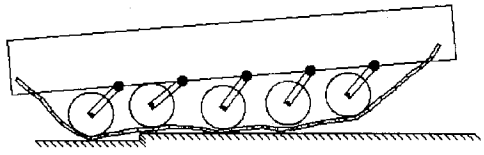

Fig. 9 Configuration of the tracked vehicle at t=0.35 sec

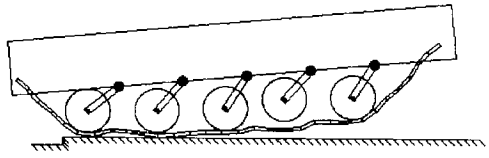

Fig. 10 Configuration of the tracked vehicle at t=0.45 sec

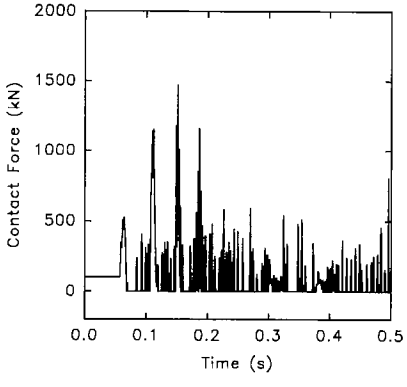

Fig. 11 Variation of the vertical contact force between the first wheel and the track

tions of the vehicle at t=0.1 sec, t=0.35 sec, and t=0.45 sec are shown in Figs. 8-10, respectively. The time histories of the vertical components of the contact forces on the first, third, and fifth road wheels acting by the track are shown in Figs. 11-13, and the detail of the vertical contact force of the first road wheel is shown in Fig. 14. As shown in the Figs. 8-14, the road wheels repeat contact and separation with the track. The time histories of the vertical acceleration of the mass center of

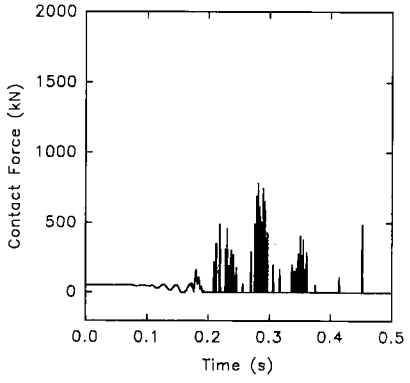

Fig. 12 Variation of the vertical contact force between the third wheel and the track

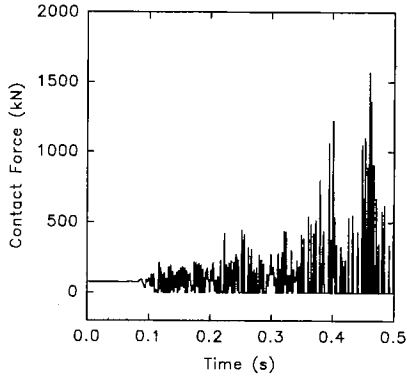

Fig. 13 Variation of the vertical contact force between the fifth wheel and the track

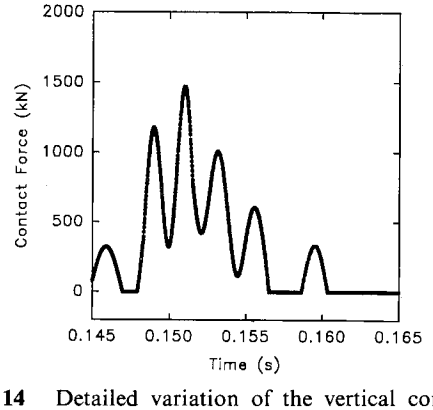

Fig. 14 Detailed variation of the vertical contact force between the first wheel and the track

the chassis is shown in Fig. 15, and the detailed variation is shown in Fig. 16. As shown in Figs. 11-16, severe oscillations develop when the vehicle passes the obstacle. The variation of the horizontal velocity of the mass center of the

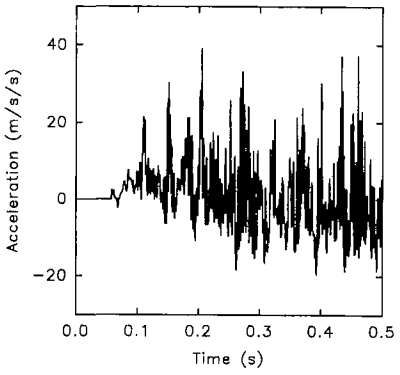

Fig. 15 Variation of the vertical acceleration of the mass center of the chassis

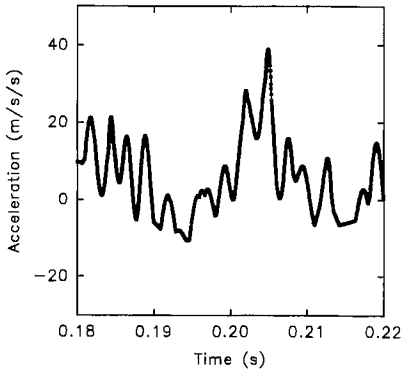

Fig. 16 Detailed variation of the vertical acceleration of the mass center of the chassis

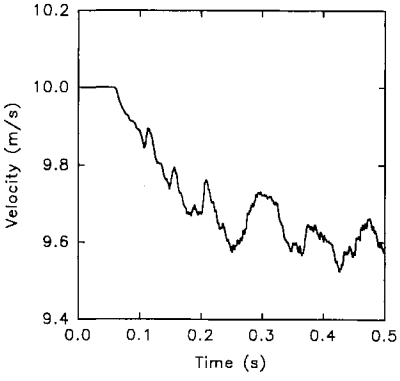

Fig. 17 Variation of the horizontal velocity of the mass center of the chassis

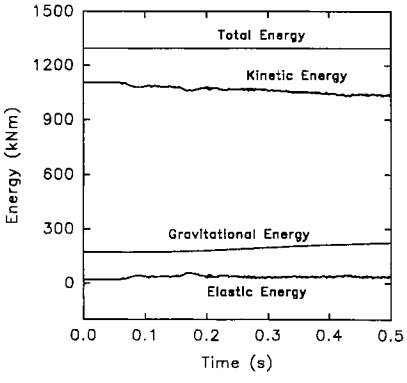

Fig. 18 Variations of the energies of the vehicle

chassis is shown in Fig. 17, which indicates that the horizontal velocity of the chassis changes when it passes the obstacle. The variation of the energies were also computed and are plotted in Fig. 18. The maximum deviation in the energy balance with respect to the initial kinetic energy remained less than 0.06% of the initial total energy, and thus it may be stated that the collision of the track with the obstacle has only negligible effect on the accuracy of the solution. Here, the energy balance is defined as

$$\text{Energy Balance} = 0.5(\dot{q}^T M_c \dot{q} + \dot{a}^T M_T \dot{a}) + \text{Elastic Energy} - \text{External Work}$$

where the elastic energy consists of the energies of the torsion bars, track tension and contact forces on the upper and lower surfaces of the track (for a similar definition of energy balance, see the references such as Vu-Quoc and Olsson(1989)).

In all of the above computations of this example, subroutine DOPRIN (Hairer, Norsett, and Wanner, 1987) was employed for the time integrations of Eq. (9) after several modifications and the integration tolerance was set to be 10^{-8}m. And the constraint tolerances for constraint error vectors in Eqs. (12), (13), and (14) were taken to be 10^{-9}m, $10^{-9}/\Delta t$ m/s, and $10^{-9}/\Delta t^2$m/s^2, respectively.

6. Concluding Remarks

A numerical technique for the dynamic analysis of a high-speed military tracked vehicle moving on a ground obstacle has been presented with special emphasis on the impulsive contact forces acting on the track. To compute the complicated dynamic contact force acting impulsively, the track has been modeled as numerous elastic links interconnected by pin joints. The mass of each

track link, the elastic elongation of a track link between pin joints by the track tension, and the elastic spring effects on the upper and lower surfaces of each track link have been considered. The equations of motion of the chassis and the road wheels have been obtained with the multibody dynamics techniques using kinematic constraints between them. The contact positions and contact forces acting on the road wheels and the track as well as the track tension have been simultaneously computed with the solutions of the equations of motion of the whole vehicle system. The numerical experiments show that, even though severe oscillations develop in the vehicle components and contact forces when the vehicle moves on an obstacle with high speed, the principle of the energy balance of the whole vehicle system is successfully checked, which may be the indication of the correctness of the solution.

In this work, to check the feasibility of the solution with a relatively simple model, the contact forces on the track have been computed by assuming linear springs on the contact points. More practical solution may be obtained if nonlinear springs (e. g., forces by Hertzian contact) and damping effects are considered and if more complicated vehicle components such as sprocket and idler are involved for the contact with the track. Also, with reasonable models of the ground deformation, the more realistic contact forces between the track and the ground may be obtained. Further work is required to compute the dynamics of the real tracked vehicles with more complicated models.

References

Addison, C. A., Enright, W. H., Gaffney, P. W., Gladwell, I., and Hanson, P. M., 1991, "Algorithm 687-A Decision Tree for the Numerical Solution of Initial Value Ordinary Differential Equations," *ACM Transactions on Mathematical Software*, Vol. 17, pp. 1～10.

Cash, J. R. and Karp, A. H., 1990, "A Variable Order Runge-Kutta Method for Initial Value Problems with Rapidly Varying Right-Hand Sides," *ACM Transactions on Mathematical Software*, Vol. 16, pp. 201～222.

Garcia de Jalon, J. and Bayo, E., 1994, *Kinematic and Dynamic Simulation of Multibody* Systems, Springer-verlag, New York.

Hairer, E., Norsett, S. P., and Wanner, G., 1987, *Solving Ordinary Differential Equations* 1, Springer-verlag, Berlin Heidelberg.

Lee, K., 1993, "An Accelerated Iterative Method for the Dynamics of Constrained Multibody Systems," *Computational Mechanics*, Vol. 12., pp. 27～38.

Lee, K., 1997, "A Numerical Method for Dynamic Analysis of Vehicles Moving on Flexible Structures Having Gaps," *International Journal for Numerical Methods in Engineering*, 40, pp. 511～531.

Lee, K., 1989, "An Accelerated Iterative Method for Contact Analysis," *International Journal for Numerical Methods Engineering*, 28, pp. 279～293.

McCullough, M. K. and Haug, E. J., 1986, "Dynamics of High Mobility Track Vehicles," *ASME J. Mechanisms Transmissions, and Automation in Design*, Vol. 108, pp. 189～196.

Nakanishi, T. and Shabana, A. A., 1994, "Contact Forces in the Non-linear Dynamic Analysis of Tracked Vehicles," *International Journal for Numerical Methods Engineering*, Vol. 37. pp. 1251～1275.

Vu-Quoc, L. and Olsson, M., 1989, "A Conputational Procedure for Intercation of High -Speed Vehicles on Flexible Structures Without Assuming Known Vehicle Nominal Motion," "Computer Methods in Applied Mechanics and Engineering, Vol. 76, pp. 207～244.

Vu-Quoc, L. and Olsson, M., 1989, "Formulation of a Basic Building Block Model for Interaction of High-Speed Vehicles on Flexible Structures," *ASME Journal of Applied Mechanics*, Vol. 56, pp. 451～458.

Appendix

For efficient computation of the iterative scheme, the acceleration technique shown by Lee (1989, 1993, 1997) is employed in this work, and

only the necessary matrices are outlined here. From matrix C, a series of matrices, C_n, are defined as

$$C_n = C / \|C\|_\infty \text{ if } n=1$$
$$= C_{n-1}(b_n I - C_{n-1}) \text{ if } n \geq 2 \quad \text{(A1)}$$

where

$$b_n = \varepsilon_{n-1} + w_{n-1} \quad (n \geq 2) \quad \text{(A2)}$$

$$w_n = 1 \text{ if } n=1$$
$$= (b_n)^2 / 4 \text{ if } n \geq 2 \quad \text{(A3)}$$

$$\varepsilon_n = \overline{\varepsilon_1} \text{ if } n=1$$
$$= \varepsilon_{n-1} w_{n-1} \text{ if } n \geq 2 \quad \text{(A4)}$$

In the above, n is an integer number and $\overline{\varepsilon_1}$ is the assumed minimum positive eigenvalue of matrix C_1. And matrix A_n is defined as

$$A_n = I \text{ if } n=1$$
$$= (b_n I - C_{n-1}) A_{n-1} \text{ if } n \geq 2 \quad \text{(A.5)}$$

And the following relation is derived by definitions (A1) and (A5):

$$C_n = C / \|C\|_\infty A_n \quad \text{(A6)}$$